Available online at www.sciencedirect.com
ScienceDirect
Trans. Nonferrous Met. Soc. China 20(2010) 637−642
Transactions of Nonferrous Metals Society of China
www.tnmsc.cn

Ni nanocomposite films formed by Ni nanowires embedded in Ni matrix using electrodeposition

ZHOU Zhao-feng(周兆锋)[1, 2], PAN Yong(潘 勇)[1, 2], LEI Wei-xin(雷维新)[1, 2]

1. Faculty of Materials, Optoelectronics and Physics, Xiangtan University, Xiangtan 411105, China;
2. Key Laboratory of Low Dimensional Materials and Application Technology, Ministry of Education, Xiangtan University, Xiangtan 411105, China

Received 10 March 2009; accepted 28 April 2009

Abstract: Ni nanocomposite films formed by Ni nanowires embedded in Ni matrix (Ni nanowire/Ni composite films) were fabricated by electrodeposition combined with supersonic stirring in a conventional Watts' bath containing Ni nanowires with diameter about 30 nm. The deposition temperature-dependent microstructure, crystal orientation, lattice constant and corrosion behavior of the Ni nanowire/Ni composite films were investigated by field emission scanning electron microscope, X-ray diffraction and potentiodynamic polarization tests, respectively. And the possible mechanism was discussed. It is found that to some extent, the deposition temperature has an impact on the microstructure, crystal orientation, lattice constant and corrosion property of the Ni nanowire/Ni composite films. The Ni nanowire/Ni composite films prepared at 50 ℃ exhibit a novel inter-twisted-nanowire microstructure and have the best corrosion resistance.

Key words: nickel nanowire; composite film; electrodeposition; corrosion resistance

1 Introduction

Metal/nanoparticle composite films have attracted tremendous interest in both fundamental study and practical applications owing to their unique and fascinating properties[1−4]. Among the available fabrication techniques, electrodeposition has become the most important one for co-depositing fine particles of metallic, no-metallic compounds or polymers in the plated layer to improve materials' performance such as wear resistance[5−6], lubrication[7] and/or corrosion resistance[8].

With the increasing availability of nanoparticles, the interest of low-cost and low temperature nanocomposite electroplating is continuously growing in the past decade. In particular for nickel matrix electrodeposition, a great variety of particles have been used such as SiO_2[9], Al_2O_3[10], ZrO_2[11], TiO_2[12] and SiC[13−14]. During the co-deposition process, these insoluble materials are suspended in a conventional plating electrolyte and captured in the growing metal films. These insoluble particles can be powder, encapsulated particles or nanowires. But to date, researches on nanocomposite films are focused mostly on particles or powders and rarely on metal nanowires or nanofibers. Only some researchers[15−17] have reported some nanocomposite films including carbon nanotubes. Additionally, insoluble particles and matrix in the references are definitely two different materials. In the present study, we added nickel nanowires to Watts' electrolyte and succeeded in fabricating the Ni nanowire/Ni composite films by electrodeposition. We also investigated the novel microstructure and corrosion properties of the as-prepared Ni nanowire/Ni composite films.

2 Experimental

Ni nanowire/Ni composite films were electrodeposited from an organic free Watts' nickel electrolyte including suspended Ni nanowires with the diameter of about 30 nm and the length of about 1 μm. The Ni nanowires were fabricated by electrodepositing nickel into the anode aluminium oxide (AAO) template.

Foundation item: Project(2008GK2001) supported by Natural Science Foundation of Hunan Province, China; Project(10772157) supported by the National Natural Science Foundation of China; Project(06C839) supported by the Scientific Research Fund of Hunan Provincial Education Department, China

Corresponding author: PAN Yong; Tel/Fax: +86-731-58298399; E-mail: ypan@xtu.edu.cn

DOI: 10.1016/S1003-6326(09)60191-6

The detailed process has been reported in some references[18−20]. The dispersed Ni nanowires (see Fig.1) were obtained by dissolving the AAO template in 2 mol/L NaOH solution. The plating bath for preparing the Ni nanowire/Ni composite films is composed of 200 g/L $NiSO_4$, 50 g/L $NiCl_2$, 40 g/L H_3BO_3 and 0.43 g/L Ni nanowires. The Ni nanowires were separated and suspended in the electrolyte by ultrasonic stirring (40 kHz, 100 W) instead of surfactant because the ultrasonic agitation is more effective on the dispersion of the particles to be co-deposited[21−22]. The electrolyte temperature was maintained by an automatic controller at a desired value (40, 50, 60 and 70 ℃) in the water bath of the ultrasonic machine (KQ2200DB). And the experiments were conducted at the current density of 25 mA/cm^2 controlled by a potentiostat/galvanostat meter (DF1731SL2A). A Ni plate of 30 mm×80 mm was used as the anode, and a copper plate of 30 mm×25 mm was used as the cathode substrate to be plated. Before the deposition, the copper plate was sequentially cleaned in acetone and distilled water, and then activated in 5% H_2SO_4 solution for 30 s. The electrodeposition was carried out for 6 min. The Ni nanowire/Ni composite films deposited at 40, 50, 60 and 70 ℃ were named as Com40, Com50, Com60 and Com70, respectively.

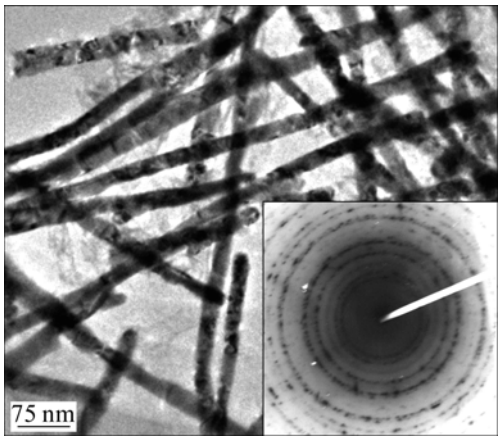

Fig.1 HRTEM image of Ni nanowires made by electro-deposition in AAO template (Inset is diffraction pattern of dispersed Ni PNW)

The morphologies of the as-prepared Ni nanowire/Ni composite films were characterized by a field emission scanning electron microscope (FESEM, LEO-1525). The phase structures were analyzed by an X-ray diffractometer (XRD, 15-100D/ Max-EAX) with Cu K_α radiation. And the corrosion properties of the composite films were studied by duplicate polarization experiments conducted on an electrochemical workstation (SI1287, Solartron, UK). A platinum electrode and a saturated calomel electrode (SCE) were used as the counter and reference electrode, respectively. Measurements were performed in 5% NaCl solutions at the temperature of 20 ℃. Anodic Tafel slope (β_a) and cathodic Tafel slope (β_c) were determined from different samples by scanning the potential at 10 mV/s from −200 to 200 mV (vs E_{corr}). Linear polarization experiments were also conducted by scanning the potential at 0.1 mV/s from −15 to 15 mV (vs E_{corr}) in order to determine the value of the polarization resistance (R_p).

3 Results and discussion

Fig.2 shows the FESEM images of the as-electrodeposited Ni nanowire/Ni composite films at different electrolyte temperatures. From Fig.2(a), it can be seen that the surface of the Com40 film is similar to the common nickel film. This suggests that the temperature of 40 ℃ is too low for the Ni crystals to form and grow as soon as possible. As a result, the nanowires cannot be snapped in time by the Ni crystals to the cathode substrate for co-deposition. Only a few of undetected nanowires and a large amount of reductive Ni atoms can reach the substrate to form the film.

An interesting picture of Com50 is shown in Fig.2(b). It can be seen that the composite film is just like a close-knit net with inter-twisted nanowires whose diameter is a little larger than the original Ni nanowires of 30 nm (Fig.1). After careful observation, it can be seen that the film is composed of a large number of micro-balls being made of nanowires. There are also several micro-balls separately adhering to the composite film and have not yet gathered into a layer. We assumed that the Ni nanowires are too thin and have too high surface energy for the ultrasonic stirring to make them apart completely. Therefore, a number of the nanowires wrap and adhere to each other for reducing their system energy and form a micro-ball suspended in the electrolyte under the effect of the ultrasonic stirring as shown in Fig.3(a). The temperature of 50 ℃ is high enough for the solution flowing quickly and sending these micro-balls to the cathode substrate as shown in Fig.3(b). The properly high temperature also helps the Ni crystals form quickly and catch the micro-balls in time. After reaching the substrate, these micro-balls further move on and adhere tightly to each other to form a close-knitted nanowire net as shown in Fig.3(c).

Fig.2(c) shows the FFSEM image of Com60 film, from which the inter-twisted wires cannot be seen clearly. It can be seen from Fig.2(c) that the nanowires grow larger and are covered by a layer of thin film. This suggests that the temperature of 60 ℃ is very high and the over potential of the cathode becomes lower. As a result, the existing nickel crystals grow more quickly. On

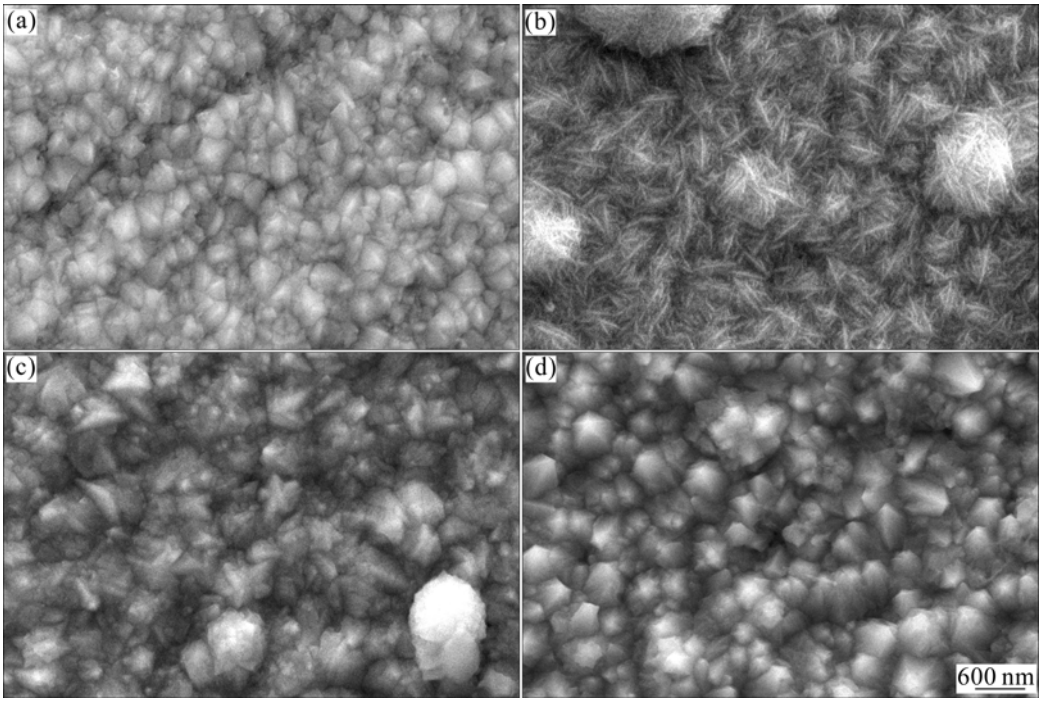

Fig.2 FESEM images of Ni nanowire/Ni composite films electrodeposited at different electrolyte temperatures: (a) 40 ℃; (b) 50 ℃; (c) 60 ℃; (d) 70 ℃

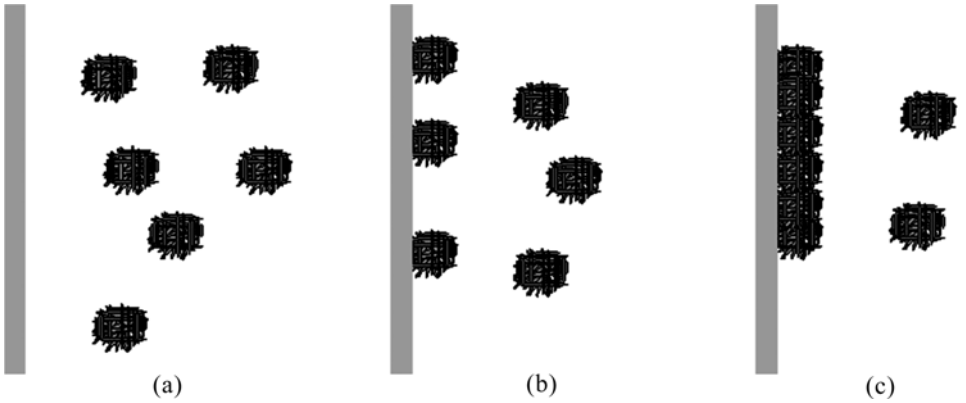

Fig.3 Schematic diagrams for formation of inter-twisted-nanowire microstructure: (a) A number of nanowires wrap and adhere to each other to form micro-balls suspended in electrolyte; (b) Micro-balls are sent to cathode substrate by quickly flowing solution; (c) Micro-balls further adhere tightly to each other after reaching substrate to form an inter-twisted-nanowire microstructure

the other hand, the surface of nanowire absorbs less positive ions under higher temperature according to the Langmuir adsorption theory[23]. So, the nanowires adhering to the substrate become less. Therefore, the growth rate of the nickel crystals gets faster than the move rate of the nanowires from the electrolyte to the cathode substrate. The reductive nickel atoms adhere to the existing nanowires and make the nanowires grow thicker. Ultimately, the nanowires, being covered by a layer of nickel film, cannot be seen distinctly.

Fig.2(d) shows the FESEM image of Com70 film. Nearly no nanowire can be seen. The Ni crystals grow up forming a smooth surface. Only large nickel crystals with the similar size of the micro-balls (see Fig.2(b)) are visible.

Fig.4 shows the XRD patterns of the four different Ni nanowire/Ni composite films and the common Ni film electrodeposited at 50℃ and the same other parameters for comparison. Though the Ni nanowires in amorphous AAO template has a preferential orientation of (111) by the XRD test[24], their adding into the electrolyte decreases the (111) peak intensity of the composite films compared with the common one. The (311) peak becomes lower for all the samples too. Other peaks of the four samples also show different intensities from the common one. Com40 has the similar XRD pattern with

the common Ni film, which is in good accordance with the result of the FESEM image. To a certain extend, the deposition temperature has an impact on the crystal orientation of the Ni nanowire/Ni composite films. The interiar mechanism needs further investigation.

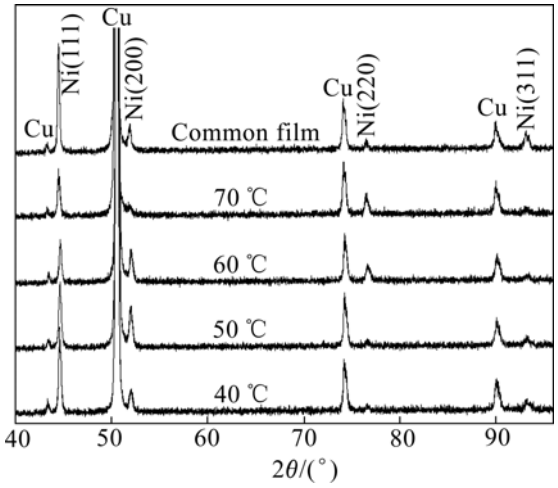

Fig.4 XRD patterns of common Ni film and Ni/Ni nanowire composite films deposited at different temperatures

From Fig.4, we can also get $d_{(111)}$ and calculate out the lattice constants of all the samples. The results are shown in Table 1. Compared with the standard $d_{(111)}$ and lattice constants of Ni, the $d_{(111)}$ and lattice constants of all the samples become smaller, agreeing with the prediction of the bond-order-length-strength (BOLS) theory[25]. The BOLS theory indicates that if the coordination number (CN) of an atom is reduced, the ionic and metallic radius of the atom would shrink spontaneously. Therefore, the CN imperfection will shorten the remaining bonds of the under-coordinated atom. In our work, all the samples have much smaller grains and plenty of boundaries where there are more under-coordinated atoms. As a result, a large amount of remaining bonds become shorter, which leads to the reduction of the lattice constant. We can also find that when the temperature is lower than 70 ℃, the $d_{(111)}$ and the lattice constant decrease with the increase of the temperature; but when the temperature reaches 70 ℃, $d_{(111)}$ increases abruptly. It is possible because the lattice will relax under higher temperature.

Table 1 $d_{(111)}$ and lattice constants of Ni nanowire/Ni composite films deposited at 40, 50, 60, and 70 ℃

Sample	d(111)/Å	Lattice constant/Å
Com40	2.027 5	3.512 6
Com50	2.027 3	3.512 3
Com60	2.024 7	3.507 8
Com70	2.032 2	3.520 8
Standard	2.034 4	3.523 0

In order to analyze the temperature-dependant corrosion resistance of the Ni nanowire/Ni composite films, potentiodynamic polarization tests were conducted on the electrochemical workstation. Fig.5 shows the measured Tafel plots. Table 2 illustrates the resulting anodic (β_a) and cathodic (β_c) Tafel slopes of all samples. The polarization resistance (R_p) was determined from the slope of the polarization resistance curves (not presented here). The determination of the corrosion rates was carried out using the following Stern-Geary equation:

$$J_{corr} = \frac{\beta_a \times \beta_c}{2.303 \times R_p(\beta_a + \beta_c)} \quad (1)$$

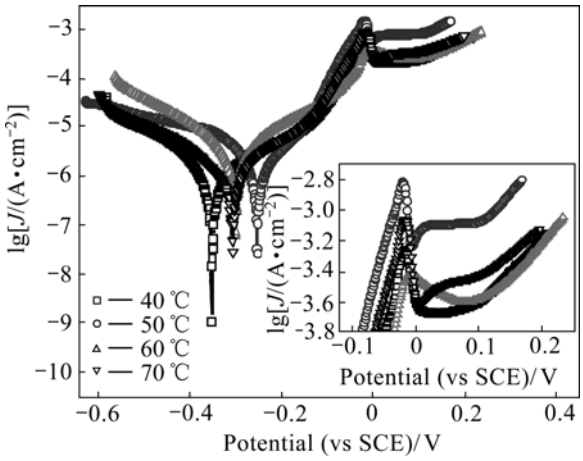

Fig.5 Tafel curves of Ni nanowire/Ni composite films deposited at different temperatures

Table 2 Corrosion rate of as-deposited Ni nanowire/Ni composite films in 5% NaCl at 20 ℃

Sample	β_a/ (mV·decade^{-1})	β_c/ (mV·decade^{-1})	R_p/ (Ω·cm^{-2})	J_{corr}/ (μA·cm^{-2})
Com40	263.83	214.38	25 861.0	1.949
Com50	252.46	170.74	27 973.0	1.612
Com60	211.57	203.53	6 315.7	7.132
Com70	182.16	219.95	21 108.0	2.050

From Table 2 we can see that the Com50 film has the lowest J_{corr} and the best corrosion resistance.

During the cathodic polarization, the only feasible reaction is the evolution of hydrogen from water reduction[26]. With the potential increasing in the anodic direction, Ni dissolution take place and the oxide or hydrated oxide is formed on the composite films, which served as the passive layers. YOUSSEF et al[26] reported that the passive film formation on the corroded surface is diffusion controlled. Com50 film has smaller

grain size and more grain boundaries. So the diffusion rate of elements in Com50 film is much higher than others. So, the corrosion resistance of Com50, which is due to the formation of passive film, is higher than others[27]. In addition, the passivation first starts on lattice defects of surface crystalline. Com50 has a high density of grain boundaries and dislocations, therefore, the Com50 film has a high density of nucleation sites for passive films, which leads to a high fraction of passive layers and low corrosion rates[28].

The inset in Fig.5 shows the locally enlarged polarization curves, which shows the passivation condition of the samples. There is a noticeable change in the passive current density for Com50 film which exhibits higher passive current density compared with others. This is because the defective nature of the passive film that forms on the Com50 film[29]. More defects are presented in the passive films of nanocrystalline film than coarse-grain one[30]. The condition is the same with the Com50 film which contains smaller grains and larger number of atoms in the boundaries. Ni cations' diffusion through a more defective film is easier, which leads to higher passive current densities in the passive range.

According to the literatures regarding the composite films made by electrodeposition, the nanoparticles are about 50 nm or larger in size and the contents of these particles in electrolyte are usually more than 1 g/L[6, 29]. These particles often agglomerate and cannot distribute uniformly[9, 30]. In the present work, the nanowire has a diameter as small as 30 nm and a length of 1μm. The content of the nanowires in the electrolyte is only 0.43 g/L, which is much less than the references. Because of the smaller sizes, the number of nanowires per unit volume is not less than that of larger particles as reported. Using these nanowires as the second phase of the co-deposited composite films has not been reported. Furthermore, the Ni nanowire/Ni composite films deposited at the temperature of 50 ℃ shows a homogeneous inter-twisted wire film, confirming that ultrasonic stirring is available for dispersing nanowires in the electrolyte[31−32]. All these swell our confidence in the next work.

4 Conclusions

1) Ni nanowire/Ni composite films have been successfully fabricated by an electrodeposition technique with the content of 0.43 g/L Ni nanowires, current density of 25 mA/cm^2 and temperatures of 40−70 ℃.

2) To some extent, the deposition temperature has an impact on the microstructure, crystal orientation, lattice constant and corrosion property of the Ni nanowire/Ni composite films.

3) The composite film deposited at 50 ℃ has a novel inter-twisted-nanowire microstructure with the best corrosion resistance.

References

[1] AYYAR A, CHAWLA N. Microstructure-based modeling of the influence of particle spatial distribution and fracture on crack growth in particle-reinforced composites [J]. Acta Materialia, 2007, 55: 6064−6073.

[2] TANAKA D A P, TANCO M A L, NAGASE T, OKAZAKI J, WAKUI Y, MIZUKAMI F, SUZUKE T M. Fabrication of hydrogen-permeable composite membranes packed with palladium nanoparticles [J]. Advanced Materials, 2006, 18: 630−632.

[3] STROUMBOULI M, GYFTOU P, PAVLATOU E A, SPYRELLIS N. Codeposition of ultrafine WC particles in Ni matrix composite electrocoatings [J]. Surface and Coatings Technology, 2005, 195: 325−332.

[4] MALFATTI C F, VEIT H M, MENEZES T L, FERREIRA Z J, RODRIGUES J S, BONINO J P. The surfactant addition effect in the elaboration of electrodeposited NiP-SiC composite coatings [J]. Surface and Coatings Technology, 2007, 201: 6318−6324.

[5] GHORBANI M, MAZAHERI M, AFSHAR A. Wear and friction characteristics of electrodeposited graphite-bronze composite coatings [J]. Surface and Coatings Technology, 2005, 190: 32−38.

[6] WANG Y, XU Z. Nanostructured Ni-WC-Co composite coatings fabricated by electrophoretic deposition [J]. Surface and Coatings Technology, 2006, 200: 3896−3902.

[7] SHI L, SUN C F, ZHOU F, LIU W M. Electrodeposited nickel-cobalt composite coating containing nano-sized Si_3N_4 [J]. Materials Science and Engineering A, 2005, 397: 190−194.

[8] GARCIA I, CONDE A, LANGELAAN G, FRANSAER J, CELIS J P. Improved corrosion resistance through microstructural modifications induced by codepositing SiC-particles with electrolytic nickel [J]. Corrosion Science, 2003, 45: 1173−1189.

[9] WANG S C, WEI C J. Kinetics of electroplating process of nano-sized ceramic particle/Ni composite [J]. Materials Chemistry and Physics, 2003, 78: 574−580.

[10] CHANG L M, AN M Z, GUO H F, SHE S Y. Microstructure and properties of Ni-Co/nano-Al_2O_3 composite coatings by pulse reversal current electrodeposition [J]. Applied Surface Science, 2006, 253: 2132−2137.

[11] HOU F Y, WANG W, GUO H T. Effect of the dispersibility of ZrO_2 nanoparticles in Ni-ZrO_2 electroplated nanocomposite coatings on the mechanical properties of nanocomposite coatings [J]. Applied Surface Science, 2006, 252: 3812−3817.

[12] LI J, SUN Y, SUN X, QIAO J. Mechanical and corrosion-resistance performance of electrodeposited titania-nickel nanocomposite coatings [J]. Surface and Coatings Technology, 2005, 192: 331−335.

[13] BENEA L, BONORA P L, BORELLO A, MARTELLI S. Wear corrosion properties of nano-structured SiC-nickel composite coatings obtained by electroplating [J]. Wear, 2002, 249: 995−1003.

[14] MING D G. Electrochemical deposition of nickel/SiC composites in the presence of surfactants [J]. Materials Chemistry and Physics, 2004, 87: 67−74.

[15] SHI L, SUN C F, GAO P, ZHOU F, LIU W M. Electrodeposition and characterization of Ni-Co-carbon nanotubes composite coatings [J]. Surface and Coatings Technology, 2006, 200: 4870−4875.

[16] CHEN X H, CHEN C S, XIAO H N, CHENG F Q, ZHANG G, YI G

J. Corrosion behavior of carbon nanotubes-Ni composite coating [J]. Surface and Coatings Technology, 2005, 191: 351−356.

[17] ARAI S, ENDO M. Various carbon nanofiber-copper composite films prepared by electrodeposition [J]. Electrochemistry Communications, 2005, 7: 19−22.

[18] MASSUDA H, FUKUDA K. Ordered metal nanohole arrays made by a two-step replication of honeycomb structures of anodic alumina [J]. Science, 1995, 268: 1466−1468.

[19] JESSENSKY O, MULLER F, GOSELE Y. Self-organized formation of hexagonal pore arrays in anodic alumina [J]. Applied Physics Letters, 1998, 72: 1173−1175.

[20] NIELSCH K, MULLER F, LI A P, GOSELE U. Uniform nickel deposition into ordered alumina pores by pulsed electrodeposition [J]. Advanced Materials, 2000, 12: 582−586.

[21] KUO S L, CHEN X L, CHEN Y C. CHIN J. Physical and chemical dispersion effects on the preparation of Ni-Al_2O_3 composite coating [J]. Journal of the Chinese Institute of Chemical Engineers, 2003, 34: 393−398.

[22] REZRAZI M, DOCHE M L, BERCOT P, HIHN J Y. Au–PTFE composite coatings elaborated under ultrasonic stirring [J]. Surface and Coatings Technology, 2005, 192: 124−130.

[23] LANGMUIR I. The constitution and fundamental properties of solids and liquids [J]. Journal of the American Chemical Society, 1916, 38: 2221−2295.

[24] ZHOU Z F, ZHOU Y C, PAN Y, WANG X G. Growth of the nickel nanorod arrays fabricated using electrochemical deposition on anodized Al temperatures [J]. Materials Letters, 2008, 62: 3419−3421.

[25] SUN C. Size dependence of nanostructures: Impact of bond order deficiency [J]. Progress in Solid State Chemistry, 2007, 35: 1−159.

[26] YOUSSEF K M S, KOH C C, FEDKIW P S. Improved corrosion behavior of nanocrystalline zinc produced by pulse-current electrodeposition [J]. Corrosion Science, 2004, 46(1): 51−64.

[27] WANG L, LIN Y, ZENG Z, LIU W, XUE Q, HU L, ZHANG J. Electrochemical corrosion behavior of nanocrystalline Co coatings explained by higher grain boundary density [J]. Electrochimica Acta, 2007, 52: 4342−4350.

[28] WANG L, ZHANG J, GAO Y, XUE Q, HU L, XU T. Grain size effect in corrosion behavior of electrodeposited nanocrystalline Ni coatings in alkaline solution [J]. Scripta Materialia, 2006, 55: 657−660.

[29] MISHRA R, BALASUBRAMANIAM R. Effect of nanocrystalline grain size on the electrochemical and corrosion behavior of nickel [J]. Corrosion Science, 2004, 46(12): 3019−3029.

[30] ROFAGHA R, SPLINTER S J, ERB U, MCINTYRE N S. XPS characterization of the passive films formed on nanocrystalline nickel in sulphuric acid [J]. Nanostructured Materials, 1994, 4: 69−78.

[31] WU B, XU B S, ZHANG B, LU Y H. Preparation and properties of Ni/nano-Al_2O_3 composite coatings by automatic brush plating [J]. Surface and Coatings Technology, 2007, 201: 6933−6639.

[32] CHOU M C, GER M D, KE S T, HUANG Y R, WU S T. The Ni-P-SiC composite produced by electro-codeposition [J]. Materials Chemistry and Physics, 2005, 92: 146−151.

(Edited by LI Xiang-qun)